Lecture Notes at CWB

June 20-23 2012

Bin Wang

Department of Meteorology and International Pacific Research Center, University of Hawaii at Manoa, 2525 Correa Road, Honolulu Hawaii 96822, USA
Email: wangbin@hawaii.edu

Contents

1. Equatorial waves

Basic theory shows that if weather systems are going to grow by converting potential to kinetic energy, their vertical scale, H, and horizontal scale, L, must scale as:

$$H/L \sim f/N,$$

where $f = 2\Omega \sin$ (latitude), with Ω the rotation rate of the Earth, is the Coriolis parameter and N is the buoyancy frequency, a measure of the vertical stratification of the atmosphere. In middle latitudes this gives an aspect ratio of about 1/100. However as the equator is approached, the aspect ratio would tend to zero, so that weather systems of a fixed horizontal scale would become shallower and shallower in the vertical. This does not occur because organized deep convection rather than potential energy is the dominant energy source for tropical motion. It determines that the vertical scale for motions is essentially that of the troposphere.

When the tropical atmosphere is subject to diabatic heating, the pressure (mass) and wind fields will experience an adjustment process. Atmospheric waves play an essential role in this adjustment process. In general, these waves propagate both horizontally and vertically. The vertically propagating equatorial waves have important consequences for the circulation of the equatorial middle atmosphere (stratosphere). However, for our purpose of understanding of the tropospheric large-scale motion, it is conveniently to simplify the problem by neglecting vertical propagation and focusing on horizontally propagating waves.

As shown in Appendix A.1, tropical waves in a resting atmosphere without diabatic heating and friction can be simplified as standing waves in the vertical direction. Their vertical structure can be described by appropriate summation of a family of vertical ("normal") modes. Each vertical mode satisfies the same set of wave equations called "shallow water equation" but with different propagation speed (Eq. A.1.5).

The properties of tropical waves are primarily controlled by two fundamental geophysical parameters. One is the Earth's rotation and the other is atmospheric density stratification. The Earth's rotational effect in the tropics is most conveniently represented by assuming the Coriolis parameter f varies linearly with distance from the equator (y) so that $f = \beta y$, where $\beta \equiv df/dy = 2\Omega/a$ is the Rossby parameter where a is the radius of the Earth. The change of sign of the Coriolis parameter f at the equator results in a special class of large-scale atmospheric waves, which are trapped laterally in the equatorial region as demonstrated by Matsuno (1966). For this reason, these tropical waves are referred to as equatorial waves.

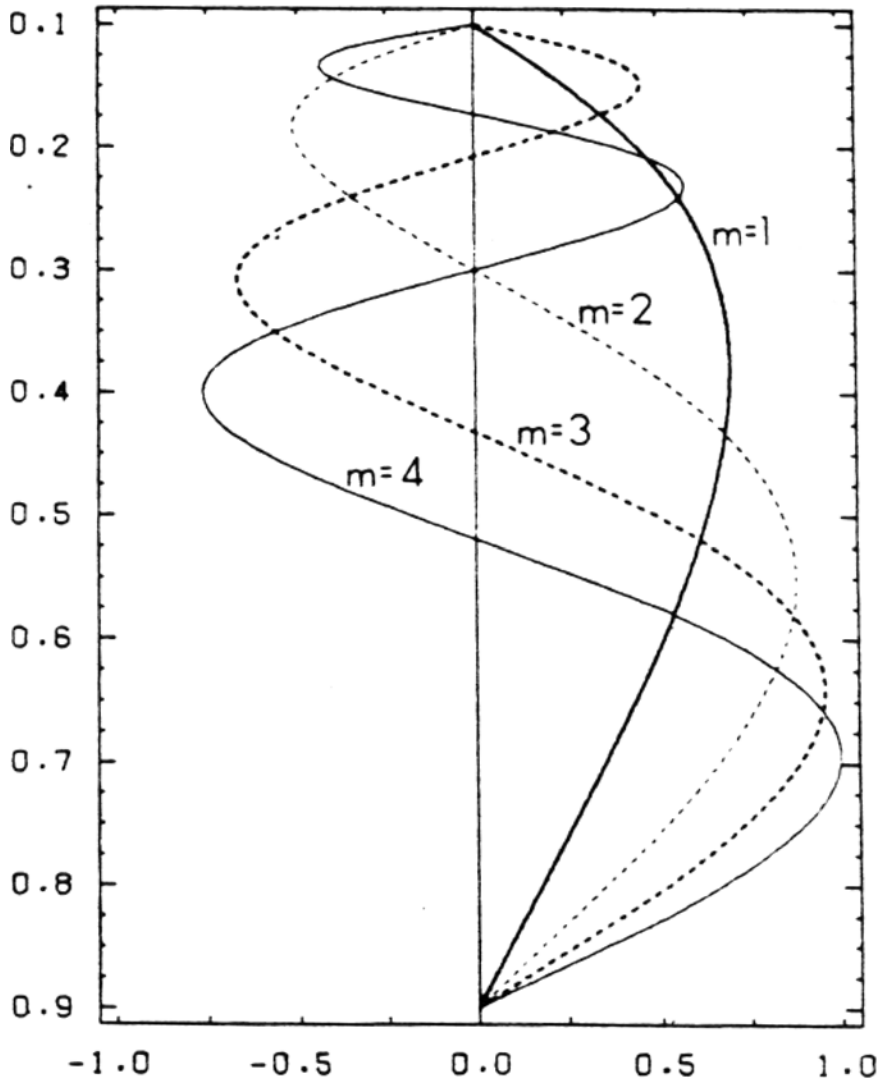

Fig. 1 Vertical structures of the vertical pressure velocity for the first four internal modes computed for an isothermal atmosphere in which the static stability parameter is proportional to the inverse of the pressure square. The vertical pressure velocity vanishes at the upper (p=0.1) and lower (p=0.9) boundary Adopted from Wang and Chen (1989).

1.1 Vertical standing modes

The atmospheric stratification determines the vertical structure of the horizontally propagating equatorial waves (Eq. A.1.6) and the corresponding gravity wave propagation speed C_0 for individual vertical mode (A.1.7). For a given typical stratification profile, the vertical velocity profiles of the lowest four vertical modes (m=1, 2, 3, and 4) are shown in Fig. 1. The gravest baroclinic mode (m=1) has maximum vertical velocity in the middle of the atmosphere. The higher baroclinic modes have more nodes and shorter wavelengths. For a typical stratification parameter value of the dry atmosphere, the phase speed computed for the lowest four vertical modes using (A.1.7) are approximately 50, 26, 18, and 13 m/s, respectively. Higher vertical modes have slower phase speeds.

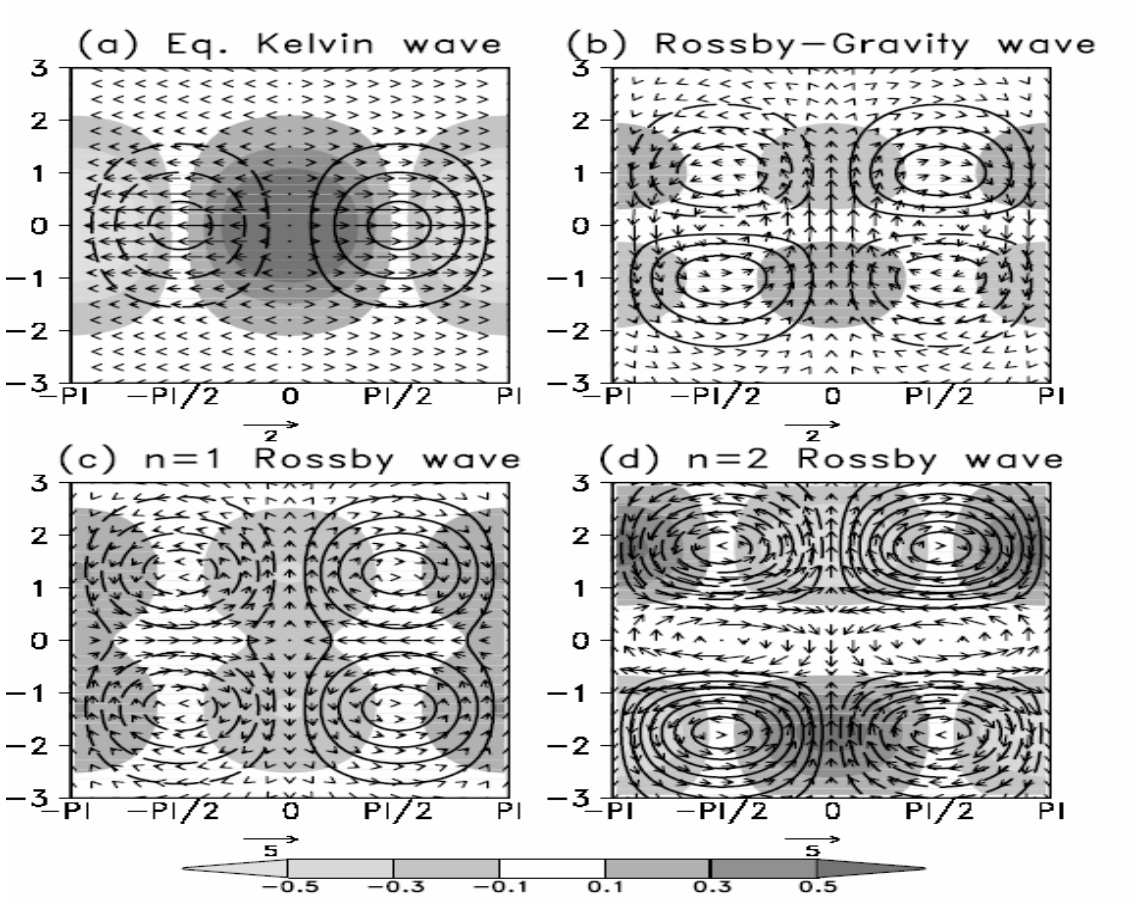

Fig. 2 Horizontal structures of the equatorial wave solution to the shallow water equations on equatorial β-plane for (a) equatorial Kelvin wave k = 1, (b) n =1 Rossby wave k = -1, (c) n =2 Rossby wave k = -1, (d) n =0 Rossby-Gravity wave k = -1. All scales and fields are dimensionless. The dimension for latitude y is the Rossby radius of deformation, $Rc = (C_0 / \beta)^{1/2}$. Contours are geopotential with interval of 0.2 units. Solid (dashed) contours are positive (negative) and zero contours are omitted. The largest wind vectors are given in the bottom-right corner. Red (blue) shading is drawn for convergence (divergence) with a 0.2 unit interval.

To the lowest order, the large-scale tropospheric motion stimulated by deep convective heating can be described by the lowest baroclinic mode (m=1) for which the internal gravity wave speed for dry atmosphere is C_0 =50 m/s. Matsuno (1966) and Gill (1980) have used the shallow water model that describes this most important vertical mode to discuss basic dynamics of the equatorial waves and atmospheric response to specified heating. The two parameters, β and $C_{0,}$ which reflect the Earth's rotational and gravitational effects, respectively, determine an equatorial trapped length scale $Rc = (C_0 / \beta)^{1/2}$ called the equatorial Rossby radius of deformation. A value of C_0 =50 m/s corresponds to an equatorial Rossby radius of deformation of about 15 degrees of latitude.

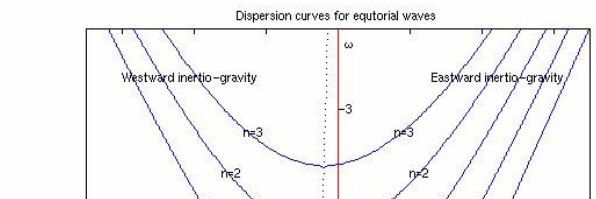

Fig. 3 Dispersion curves for equatorial waves (up to n=3) in a resting basic state as a function of nondimensional zonal wave number k and frequency ω. Positive (negative) wavenumber k means eastward (westward) propagating waves. The thick dashed curve indicates zero group velocity.

1.2. Equatorial Kelvin wave

The eastward-propagating Kelvin wave is a possible free solution to the perturbation equations of the shallow water model (A.1.5) provided that the meridional velocity vanishes or the motion is exactly in the along-equator direction. The resultant solution of the Kelvin wave is given in dimensional form by (A.2.3).

In general, the Kelvin wave is a special type of gravity wave that is affected by the Earth's rotation and trapped at the Equator or along lateral vertical boundaries such as coastlines or mountain ranges. The existence of the equatorial Kelvin wave relies on (i) gravity and stable stratification for sustaining a gravitational oscillation, (ii) significant Coriolis acceleration, and (iii) the presence of the Equator. The Coriolis force acting on a westerly flow in the equatorial region tends to turn it towards the equator in both hemispheres. This acts to pile up fluid in the equatorial region and forms a pressure maximum at the equator. The associated poleward pressure gradient force that then balances the equatorward Coriolis force, i.e. it leads to the westerly flow being geostrophic. Thus the equator acts like a lateral wall to support the Kelvin wave. The high (low) pressure is in phase with westerly (easterly) flows (Fig. 2a). The fact that the equatorial trapping demands that the pressure and westerly flow are in phase means that it works only for the eastward propagating gravity wave, which gives the unique nature of the equatorial Kelvin wave.

At the Equator, Kelvin waves always propagate eastward and have zonal velocity and pressure perturbations that decay with latitude on a scale Rc, the equatorial Rossby radius of deformation (A.2.3). Figure 2a shows the horizontal structure of the equatorially

trapped Kelvin wave solution for a simplified mode 1 vertical structure. Of note is that the Kelvin wave propagates without dispersion as for non-rotating gravity waves.

1.3 General dispersion relation

In addition to the equatorial Kelvin wave solution, other equatorial wave solutions exist. The general dispersion relation is derived in the Appendix A.2 and given by (A.2.6). The dispersion relation describes the fundamental property of the wave motion by relating the wave frequency ω and zonal wavenumber k. Here ω is assumed to be always positive so that $k>0$ implies eastward propagation relative to the ground with phase speed $C_x = \omega/k$.

Figure 3 shows schematically the dispersion relation for all types of equatorial waves derived by Matsuno (1966). The special Kelvin wave is represented by the straight line in the $k>0$ domain. The general dispersion relation reflects an infinite family of meridional modes, each associated with an integer index n. When $n \geq 1$, there are two distinct groups of waves: high frequency and low frequency waves (A.2.6). Taking $C_0 = 50\,\mathrm{ms}^{-1}$, the high frequency waves have a period shorter than 1.26 days. The low frequency waves have a period longer than 7.3 days.

1.4 Low-frequency equatorial Rossby waves and mixed Rossby-gravity waves

For low frequency waves, it is shown in Appendix A.2 that the dimensional dispersion equation (A. 2. 6) can be approximated by

$$\frac{\omega_*}{k_*} = -\frac{\beta}{k_*^2 + (2n+1)\,\beta/C_0}\,.$$

This is the same dispersion relation as a Rossby wave in a beta-plane channel except that the quantized y-wavenumber has a slightly different form due to the meridional boundary conditions. These low-frequency modes are, therefore, called *equatorial Rossby waves*. They occur because f varies with latitude. The higher the index of the meridional mode n, the lower the frequency ω.

In contrast with equatorial Kelvin waves, equatorial Rossby waves always propagate westward as shown by the negative sign in the above dispersion relation. However, the group speed, which represents the speed at which wave energy propagates, can be either eastward or westward. In the dispersion diagram Fig. 3, the slope of the dispersion curves represents the corresponding group speed. A positive slope (frequency increases with increasing wavenumber) indicates an eastward group speed. The dashed curve in Fig. 3 highlights the zero group speed. To the right hand side of the curve of the zero group speed, energy associated with Rossby waves propagates westward as indicated by the negative slope. These waves have small wave numbers or long wavelengths. Thus, the energy associated with *long Rossby waves* propagates westward while the energy associated with *short Rossby waves* propagates eastward. This property is important when considering reflection of Rossby waves at the oceanic lateral boundaries and thermocline adjustment in a finite ocean basin.

For long Rossby waves, $k \to 0$, so that $\omega/k \approx -Co/(2n+1)$ ($n = 1,2,...$), implying that they are approximately non-dispersive. The dimensional westward phase speed is $(2n+1)^{-1}$ times the long gravity wave speed C_0. Thus, the fastest long Rossby wave

(n=1) speed is about one-third of the Kelvin wave speed (and in the opposite direction).

Figures 2b and 2c depict the horizontal structure for $n=1$ and $n=2$ equatorial Rossby waves. Here the axes are in units of Rc. Rossby waves are characterized by a geostrophic relationship between pressure and the meridional as well as the zonal wind. Strong zonal winds are found near the equator for the $n=1$ mode, which is expected from approximate balance between pressure gradient and Coriolis forces (both of them approach zero as $y \to 0$). For the $n=1$ mode, zonal wind u and geopotential height ϕ are symmetric about the equator, while v is antisymmetric. On the other hand, for the $n=2$ mode, u and ϕ fields are antisymmetric about the equator but v is symmetric. At the equator, there is no meridional motion for the $n=1$ mode, while no zonal motion for $n=2$ mode. The maximum convergence/divergence are located at y=1.25 for the n=1 mode and y=1.75 for the n=2 mode.

The high frequency waves are inertia-gravity waves. The behavior of these waves is not discussed here. Interested readers are referred to Matsuno (1966).

When $n=0$, the dispersion equation $\omega^2 - k^2 - k/\omega = 1$ yields only one meaningful root $k = \omega - 1/\omega$ (the curve $n=0$ in Fig. 3). Of note is that for large ω, one has $k=\omega$, which is the asymptotic limit of high wave-number gravity waves. On the other hand, for small ω, one has $k=-1/\omega$, which is the high wavenumber limit of the Rossby waves. For this reason, this particular $n=0$ mode is called the (Mixed) Rossby-gravity wave. This mixed mode is unique in the equatorial region. The crossover point from k positive to negative, corresponds to a dimensional period of about 2.1 days for $C_0 = 50\,\mathrm{ms}^{-1}$, and represents a stationary wave in the y direction; the waves with periods shorter than 2.1 days ($k>0$) propagate eastward while waves with periods longer than 2.1 days ($k<0$) propagate westward. The energy associated with the Rossby-gravity waves, however, is always eastward (Fig. 3).

Figure 2d shows the horizontal distribution of velocity and pressure for westward moving Rossby-Gravity waves. The pressure and zonal velocity are antisymmetric about the equator while the meridional component v is symmetric. The largest meridional flow occurs at the equator (cross-equatorial flow). The largest convergence/divergence occurs at y=1.

The high frequency waves (large ω) are inertio-gravity waves. These are almost symmetric in their eastward and westward propagation.

2. Forced steady motion

The latent heat released during convection drives the atmospheric circulation while the strength and the location of convection depend on large scale circulation. In this section, this complex interaction is simplified to a one-way problem as we examine how the tropical atmosphere responds to a *given* heat source (pattern and strength).

2.1 The wave perspective

To illustrate the fundamental physical processes, Gill (1980) used a single sinusoidal vertical mode, shallow water equation model on an equatorial β-plane (Eq. A.2.1). This

simplification is based on the consideration that the heating released in the middle troposphere stimulates primarily the lowest baroclinic vertical mode. Gill considered a steady-state motion in a resting basic state forced by a given heating Q. The forced motion is sufficiently weak that it can be treated using linear dynamics. The friction takes the form of Raleigh damping (a linear drag that is proportional to wind speed) and the thermal damping takes the form of Newtonian cooling (a heating rate proportional to the temperature perturbation from its basic equilibrium state). For simplicity, the momentum and thermal damping rates are assumed to have the same time-scale, ε^{-1}, everywhere. Taking long wave approximation (i.e., neglecting the high frequency inertio-gravity waves, Gravity-Rossby waves and the short Rossby waves), the nondimensional governing equations can be then be derived from (A.2.1), which takes the following form:

$$\varepsilon u - yv = -\frac{\partial \phi}{\partial x}, \tag{2.1a}$$

$$yu = -\frac{\partial \phi}{\partial y}, \tag{2.1b}$$

$$\varepsilon \phi + (\frac{\partial u}{\partial x} + \frac{\partial v}{\partial y}) = -Q. \tag{2.1c}$$

Here Q is a nondimensional heating rate. A positive sign for Q gives u, v, ϕ at the surface of the model atmosphere. The tropopause u, v, ϕ have opposite signs from their corresponding low-level counterparts. The vertical velocity is given by (2.2)

$$\omega = -(\frac{\partial u}{\partial x} + \frac{\partial v}{\partial y}) = Q + \varepsilon \phi. \tag{2.2}$$

The analytical free wave solutions can be derived from (2.1) after replacing damping terms with local rates of change and dropping the heating term. The free wave solutions consist of equatorial Kelvin waves, long Rossby waves and the long Rossby-gravity wave. It is expected that these types of waves will adjust the geopotential and winds toward the imposed diabatic heating and reach a steady state under the damping. This steady state is the solution of (2.1).

To derive the analytical solution of (2.1), it is suffice to eliminate u and ϕ from (2.1), which leads to a single equation for v:

$$\varepsilon \frac{\partial^2 v}{\partial y^2} + \frac{\partial v}{\partial x} - \varepsilon y^2 v = y\frac{\partial Q}{\partial x} - \varepsilon \frac{\partial Q}{\partial y}. \tag{2.3}$$

The series solution for v under giving heat forcing, Q, can be expressed as

$$v(x,y) = \sum_{m=1}^{\infty} v_m(x) D_m(y), \tag{2.4a}$$

$$Q(x,y) = \sum_{m=1}^{\infty} Q_m(x) D_m(y). \tag{2.4b}$$

In (2.4) $D_m(y)$ is the Weber-Hermite function (see Eq. A.2.7a). It can be shown that the coefficients $v_m(x)$ can be solved from the following equation by assuming the coefficients for each order of m vanish:

$$\sum_{m=1}^{\infty}\left\{\begin{array}{l}\dfrac{dv_m}{dx}-\varepsilon(2m+1)v_m-\dfrac{d}{dx}\left[\dfrac{1}{2}Q_{m-1}+(m+1)Q_{m+1}\right]\\ +\dfrac{\varepsilon}{2}Q_{m-1}-\varepsilon(m+1)Q_{m+1}\end{array}\right\}=0\,. \qquad (2.5)$$

Gill presented two basic solutions, one for an equatorially symmetric isolated heating Q_s and the other for an equatorially antisymmetric dipole heating Q_{as}, i.e.,

$$Q_s(x,y)=D_0(y)F(x)=e^{-y^2/2}F(x)\,, \qquad (2.6)$$

$$Q_{as}(x,y)=Q_1(x)D_1(y)=2ye^{-y^2/2}F(x)\,, \qquad (2.7)$$

where

$$F(x)=\cos kx \qquad (\,|x|<\mathrm{L}\,)$$

$$F(x)=0 \qquad (\,|x|>\mathrm{L}\,)$$

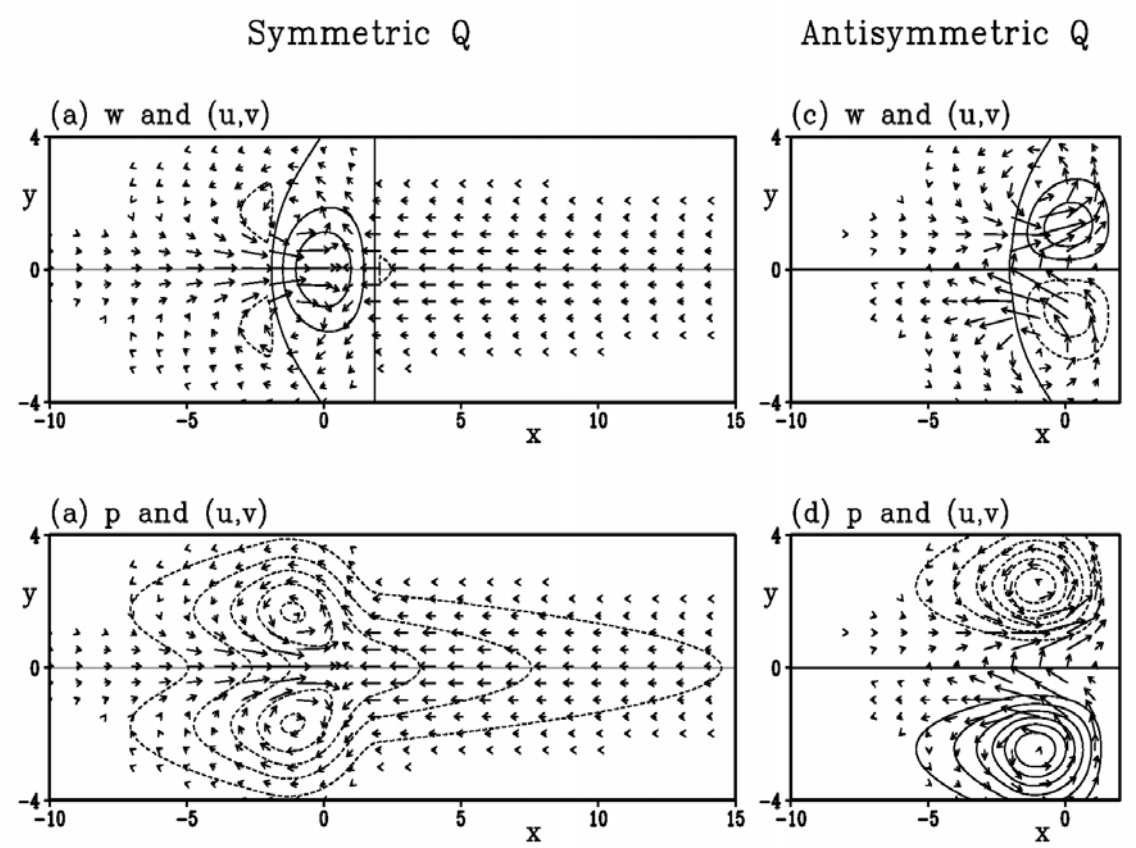

Fig. 4 Gill's solution for (a) heating symmetric about the equator, (b) heating antisymmetric about the equator.

Figures 4a and 4b show the solution of Gill model for the symmetric heating (2.6). The upward vertical motion basically coincides with the imposed heating field as implied by Eq. (2.2). Gill interpreted this circulation pattern in terms of the propagation of the large-scale equatorial Kelvin and Rossby waves. The low-level easterlies to the east of the

heating are due to a Kelvin wave propagating eastward in the presence of the damping. The low-level westerlies to the west of the heating are the result of westward propagation of the damping n=1 Rossby wave. Since the Kelvin wave has no meridional component, the easterlies are more tightly trapped to the equator. On the other hand, the Rossby wave consists of two cyclonic gyres symmetric and straddling the Equator.

Along the equator (v'≅0) Eq. (2.1) can be approximated as

$$-\varphi_x - \varepsilon u' = 0.$$

Integrating along the equator, we obtain

$$\int_0^{2\pi a} u' dx = -\int_0^{2\pi a} \varphi_x dx/\varepsilon = 0.$$

The above constraint means that the integral of the zonal wind due to the Rossby waves is balanced by the integrated zonal wind associated with the Kelvin waves. Since Kelvin waves move eastward at a speed roughly three times that of the fastest moving Rossby wave. Thus, when a steady state is reached, the damping distance of the Kelvin waves is about three times larger than the damping distances of the Rossby waves. That creates a wider region of easterly winds to the east of the heating than the westerly wind region to its west. The above equation also implies that the zonal wind associated with Rossby waves must be stronger than the zonal winds associated with Kelvin waves.

Under the long-wave approximation, Rossby waves occur only to the west of the forcing region and Kelvin waves only to the east. In the presence of the short Rossby waves, the energy of the short Rossby waves can propagate eastward because of dispersion. Also, if the damping is not too strong, the eastward propagating Kelvin waves and the westward propagating Rossby waves can travel far enough to interact with each other due to the cyclic nature of the real domain.

Figures 4c and 4d show Gill's solution for the antisymmetric heating. The major ascent and descent regions tend to coincide with imposed heating and cooling, respectively. There is a cyclonic circulation in the heated hemisphere and anticyclonic circulation in the cooled hemisphere at low-levels. In this case the excited Rossby-gravity waves are confined within the forcing region, and the Rossby waves propagate westward. There is no response to the east of the heat source because of the absence of equatorially symmetric eastward propagating Kelvin waves. Along the equator there are northerly (southerly) winds in the lower (upper) level, which means that mass transported from the cooling (heating) hemisphere to the heating (cooling) hemisphere in the lower (upper) level. A circulation pattern more relevant to the Asian summer monsoon may be obtained using a thermal forcing that is the sum of the symmetric and antisymmetric forcing. In this situation, the imposed heating field is asymmetric about the equator with the heating mainly in the northern Hemisphere. If the equatorial Rossby Radius of deformation R_c is taken to be 10^o of latitude, the solution corresponds to maximum heating at $10^\circ N$ and covering 40° of longitude. This heat source is similar to the summer monsoon heating in the Bay of Bengal to Philippines except that the latter is centered near $15^\circ N$. The solution corresponding to this "summer monsoon" heating can be obtained by adding the solution shown in Figs. 4a, and 4b and is shown in Figs. 5a and 5b.

There is a low-level cyclonic circulation in the heating hemisphere to the west of the heating, due to westward propagation of the long Rossby waves. The flow pattern to the east of the heating region is due to the eastward propagation of the Kelvin waves. Thus the winds are easterlies toward the heat source and tend to parallel to the equator and

symmetric about the equator. As stated above, they move three times faster than the long Rossby waves, and thus cover a larger longitudinal range.

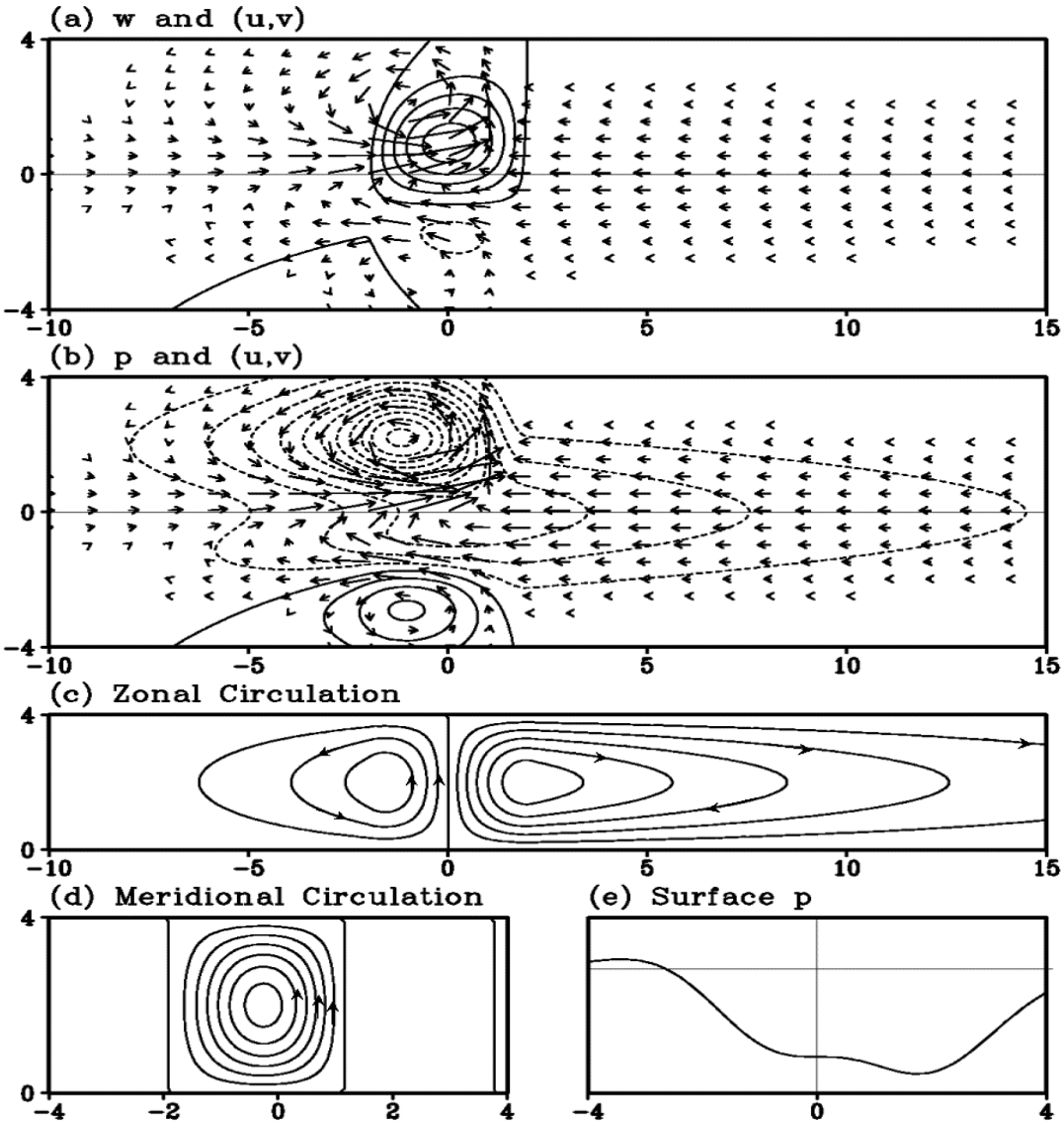

Fi n

Figs. 4a and 4b. Shown also is the zonal mean circulation and meridional mean zonal circulation.

In the Southern Hemisphere the cooling and equatorial warming induced solution shows a weak trough close to the equator and an anticyclonic circulation poleward of this. The entire circulation pattern bears close similarity to the summer circulation in the Indian-Pacific sector.

Figures 5c and 5d show the meridionally and zonally averaged circulations associated with the asymmetric heating, respectively. The meridionally averaged zonal circulation is referred to as Walker cell (Bjerknes 1966), which comprises east-west atmospheric circulation cells along the equatorial belt. Analogous to observations, the dominant

component is the Pacific branch, which consists of easterly winds at the lower troposphere, westerly winds at the upper troposphere, rising motion over the western Pacific, and subsidence over the eastern Pacific. The zonal mean meridional circulation is referred to as "Hadley cell" (Lorenz 1967). The Hadley circulation exhibits a rising branch over the NH monsoon trough latitude (the major surface low pressure) and sinking branch over the SH cooling region. It is of interest to note a secondary low pressure just south of the equator. This Hadley cell is a result of the antisymmetric component of heat forcing.

It has already been said that the longitudinal extent of the Rossby wave structures to the west and the Kelvin wave structure to the east depend on the wave speeds and the damping time scale, and that if this time-scale is not short enough there will be interference through propagation around the equator. It is also clear from 2.2 that outside the heating region, the vertical motion is totally dependent on the damping. Therefore the whole meridionally averaged structure shown in Fig. 5c, and in particular the Walker Cell, depends on the damping. The figures shown here assume a dimensional damping time-scale of about 2.5 days. It is interesting that to produce realistic pictures this simple model requires such large thermal and momentum damping, not just in the boundary layer but throughout the depth.

2.2 The vorticity and thermodynamic equation perspective

Assuming that advection by any basic state may be neglected the undamped vorticity equation may be written

$$\frac{\partial \zeta}{\partial t} + \beta v = f \frac{\partial w}{\partial z}. \tag{2.8}$$

Here ζ is the vertical component of relative vorticity, the β term represents the meridional advection of planetary vorticity and the term on the right hand side represents the creation of cyclonic (anti-cyclonic) vorticity by the stretching (shrinking) of the vorticity due to the Earth's rotation. Scale analysis shows that the thermodynamic equation may be written as

$$N^2 w = Q. \tag{2.9}$$

Here the left had side term represents adiabatic cooling (warming) due to ascent and expansion (descent and compression). The heating is again represented by Q, which would be proportional to the value used before in (2.1c).

Consider a region of large-scale, deep convective heating in the equatorial region as sketched in Fig. 6. Eq. (2.9) shows that there is ascent in the region of heating, with adiabatic cooling balancing the diabatic heating. The stretching term in the vorticity equation then implies the tendency to create cyclonic circulations in the lower troposphere and anticyclonic circulations in the upper troposphere, as shown in Fig. 6a. Under the action of the β-effect, which is described the in the vorticity equation, these circulations tend to drift westwards just as occurs in Rossby waves. The equilibrium situation is reached when they have drifted to the point shown in Fig. 6.b where there is a balance in the convective region:

$$\beta v = f \frac{\partial w}{\partial z}. \tag{2.10}$$

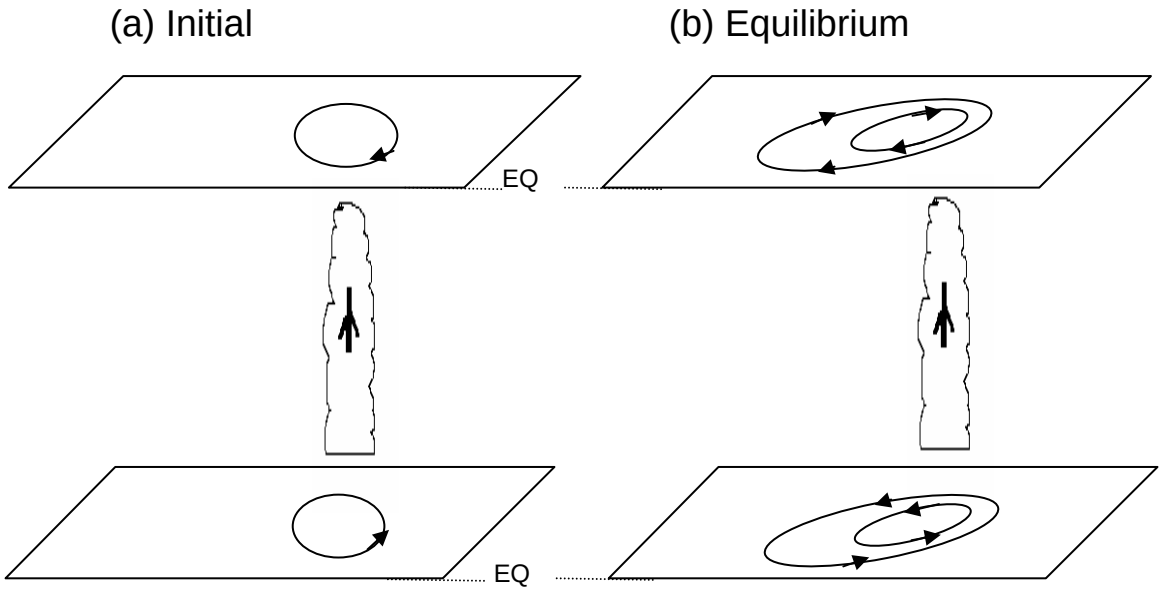

Fig. 6 Schematic diagram showing response of the tropical atmosphere to an imposed deep cumulus heating: (a) Initial tendency, and (b) equilibrium solution. If the heating were located in the Southern Hemisphere, the resultant flows would be a mirror image.

This is often referred to as Sverdrup balance. For example in the upper troposphere, the shrinking of vortex tubes is balanced by the advection of larger basic vorticity from higher latitudes. Combining Eqs. 2.9 and 2.10 leads to the approximate relationship:

$$\beta v \approx \frac{f+\varsigma}{\theta_z}\frac{\partial Q}{\partial z}. \qquad (2.11)$$

As discussed by Wu et al. (1999) and Liu et al. (2001) this form emphasizes the importance of the vertical distribution of the heating.

If the heating is away from the equator then the vortex stretching is only in that hemisphere and so the circulations are only created there.

In terms of the solutions determined using the wave approach, it is clear that the vorticity arguments have given a complementary perspective on the formation of the Rossby wave circulations to the west of the heating. For a different perspective on the Kelvin wave response to the east we take account of the cyclic nature of the equatorial domain and consider a case with zero zonally averaged heating. In this case small, uniform cooling at other longitudes compensates the local convective heating. As illustrated in Fig. 7a, the cooling then leads to descent in this region, and vortex stretching at upper levels and shrinking at lower levels. The consequent zonally elongated upper level cyclones and lower level anticyclones are dominated by westerly and easterly winds, respectively. These circulations again tend to drift westwards to give Sverdrup balance with, in the cooling region, poleward components of the winds in the upper troposphere (to the east of the heating region) and equatorward components in the lower troposphere. Damping in the vorticity equation would act to reduce the westward drift of all the circulations. The equilibrium state is shown in Fig. 7b).

These vorticity arguments give a perspective on the motions forced by large-scale deep convective heating that is complementary to that given by the wave approach. They also show the generality of the nature of the particular solutions obtained using that approach.

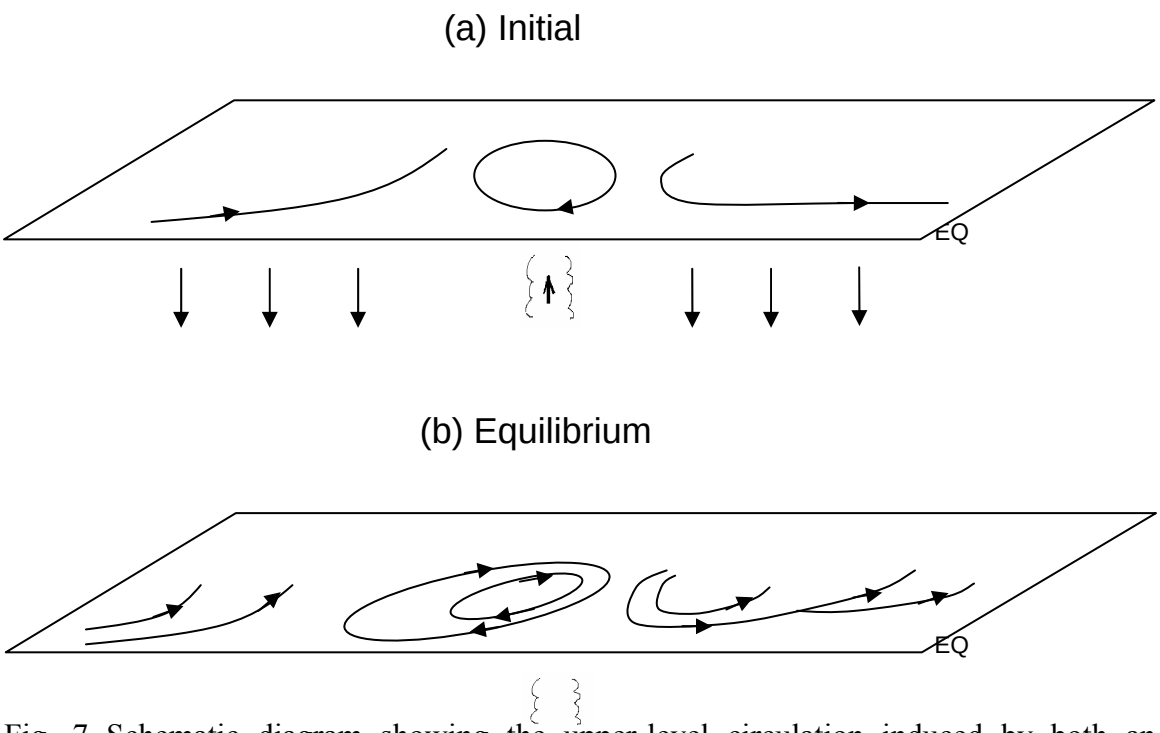

Fig. 7 Schematic diagram showing the upper-level circulation induced by both an imposed heating and the corresponding compensated cooling outside of the heating region: (a) initial tendency, and (b) equilibrium solution. The lower-level circulation would be the same except with opposite sense. If heating spreads into the Southern Hemisphere the circulation would be a mirror image.

3. Effects of mean flows on equatorial waves and forced motion

The theories of Matsuno (1966) and Gill (1980) discussed in sections 1 and 2 deal with perturbation motions in a resting environment. In reality, the equatorial waves induced by deep convective heating penetrate the entire troposphere where the three-dimensional background flows can have significant modification on the behavior of the waves. Observed anomalies associated with monsoon variability are departures from monsoon background flow. Thus, understanding of how the planetary scale background flows alter the properties of the equatorial waves is fundamental for explaining various aspects of monsoon variability.

While the tropical seasonal mean flow has a complicated three-dimensional structure, to the lowest order of approximation, one may consider a basic zonal flow, $U(y, p)$, that is in geostrophic balance and varies with height and latitude. The question to be addressed is how the meridional and vertical shears of the zonal mean flow affect the properties of the horizontally propagating low-frequency waves. The separation of variables to give a vertical mode and the shallow water equations in the horizontal is only possible for a

resting atmosphere basic state. The possible effects introduced by horizontal a vertical shears will be discussed in this section.

The likely effects of the meridional shear of such a zonal flow are suggested by the use of a modified shallow water model. The modified model would be the same as (A.1.5) except that the β-term in the zonal momentum equation should be replaced by the meridional gradient of the absolute vorticity of the basic flow, ($\beta - \partial^2 \bar{u}/\partial y^2$). Thus, the meridional shear influences the equatorial waves through latitude-dependent zonal advection (Doppler-shift) and through changing the basic state vorticity gradients. Theoretical analysis indicates that the effect of the realistic meridional shear on low-frequency waves is generally moderate. The shear-induced change of the absolute vorticity gradients makes baroclinic Rossby modes more tightly trapped near the equator (Wilson and Mak 1984). The trapping effect is significant for short waves but negligible for planetary-scale (wavenumber 1 to 4) waves (Wang and Xie 1996). The Doppler-shift effect at the latitude where the geopotential reaches maximum amplitude affects the wave propagation speed and has a major impact on the group velocity (Hoskins and Jin 1991). The meridional shear affects equatorial Kelvin waves in a way similar to that in which it affects the Rossby waves except that the Kelvin waves are more trapped near the equator if $\partial^2 \bar{u}/\partial y^2 > 0$, whereas they may be less trapped when $\partial^2 \bar{u}/\partial y^2 < 0$. The meridional shear can also make Kelvin waves become weakly dispersive due to the wavelength-dependent modification of their meridional structure and latitude-dependent zonal advection (Wang and Xie 1996).

In contrast to the effects of the meridional shear, the vertical shear of the zonal mean flow can considerably change the behavior of the equatorial waves in a resting atmosphere and atmospheric response to a given heat source without mean flows. In the presence of a summer mean flow, Webster (1972) showed that the atmospheric response in the vicinity of heat forcing has a baroclinic structure but displays a barotropic structure away from the forcing region. Kasahara and Silva Dias (1986) noticed the vertical shear of the basic flow permits a coupling of the external and internal modes. Lim and Chang (1986) demonstrated this coupling process using an f-plane model.

In this section, an idealized model on equatorial β-plane is used to examine the impacts of a vertically sheared zonal flow, *U(p)*, on low-frequency equatorial waves. In the presence of vertical shear, the different vertical modes are coupled by the shear and no longer separable. Wang and Xie (1996) have developed a simple two-level model describing equatorial waves propagating through a zonal flow with a constant vertical shear. The derivation is presented in Appendix A3.

The two-level model represents two vertical modes, a barotropic mode and a baroclinic mode (A.3.2), which are governed by Eq. (A.3.3) and (A.3.4), respectively. The barotropic mode is essentially a Rossby wave modified by a forcing arising from the baroclinic mode acting on the vertical shear. The baroclinic mode is governed by a modified shallow water equation including the feedback from the barotropic mode. The forcing terms on the r.h.s. of Eqs. (A.3.3) and (A.3.4) indicate interactions between the barotropic and baroclinic modes in the presence of vertical shear.

Linear wave solutions of the form

$$(u_-, v_-, \phi_-, \psi) = \mathrm{Re}(U, V, \Phi, \Psi) e^{i(kx-\omega t)}$$

can be shown to satisfy a set of ordinary differential equations. With Matsuno's (1966) meridional boundary conditions, one can determine the meridional structures of the barotropic and baroclinic modes and the dispersion relation can be determined.

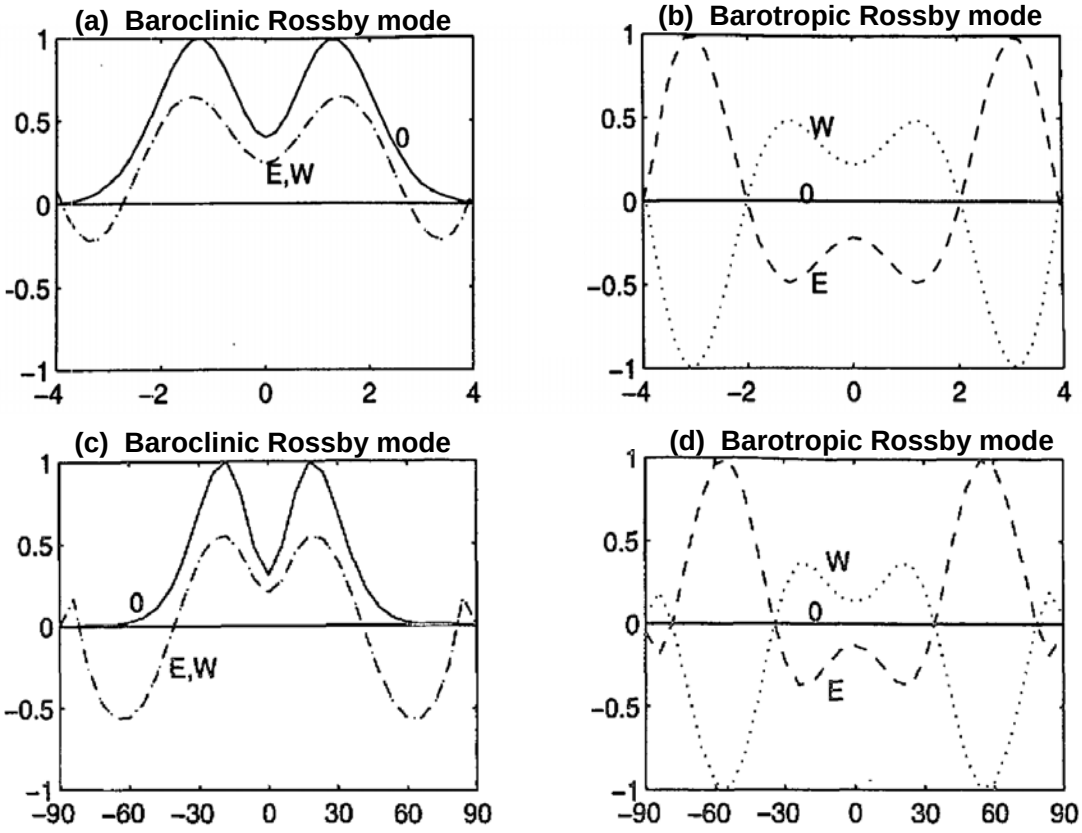

Fig. 8 Meridional structures of the geopotential field for (a) baroclinic and (b) barotropic Rossby wave mode (n=1) calculated using an equatorial β-plane. Panels (c) and (d) are the same as in (a) and (b) except computed from a spherical coordinate model (Adopted from Wang and Xie 1996).

3.1. Effects of vertical shear on the Rossby wave structure and propagation

Figure 8 shows meridional structures of the geopotential (thickness) field of the barotropic (baroclinic) modes for the n=1 (most equatorial trapped) Rossby waves. Here a westerly vertical shear means that westerly wind increases with height or easterly wind decreases with height. In the presence of the vertical shear, the baroclinic mode remains equatorially trapped (Fig. 8a). In contrast, the barotropic mode extends poleward with geopotential extremes occurring in the extratropics around three Rossby radii of deformations away from the equator (Fig. 8b). To confirm the results derived from the equatorial β-plane, a parallel analysis on the spherical coordinates was carried out (Wang and Xie 1996). The results show that the maximum geopotential perturbation of the barotropic mode is found near 57° latitude in the spherical coordinate model (Fig. 8d). Due to the feedback of the barotropic mode, the baroclinic mode also has significant amplitude around 60^o latitude (Fig. 8c).

The lowest baroclinic mode in the absence of mean flow vertical shear exhibits a precisely out-of-phase flow field in the upper and lower levels. The presence of the vertical shear modifies the vertical structure of the waves dramatically.

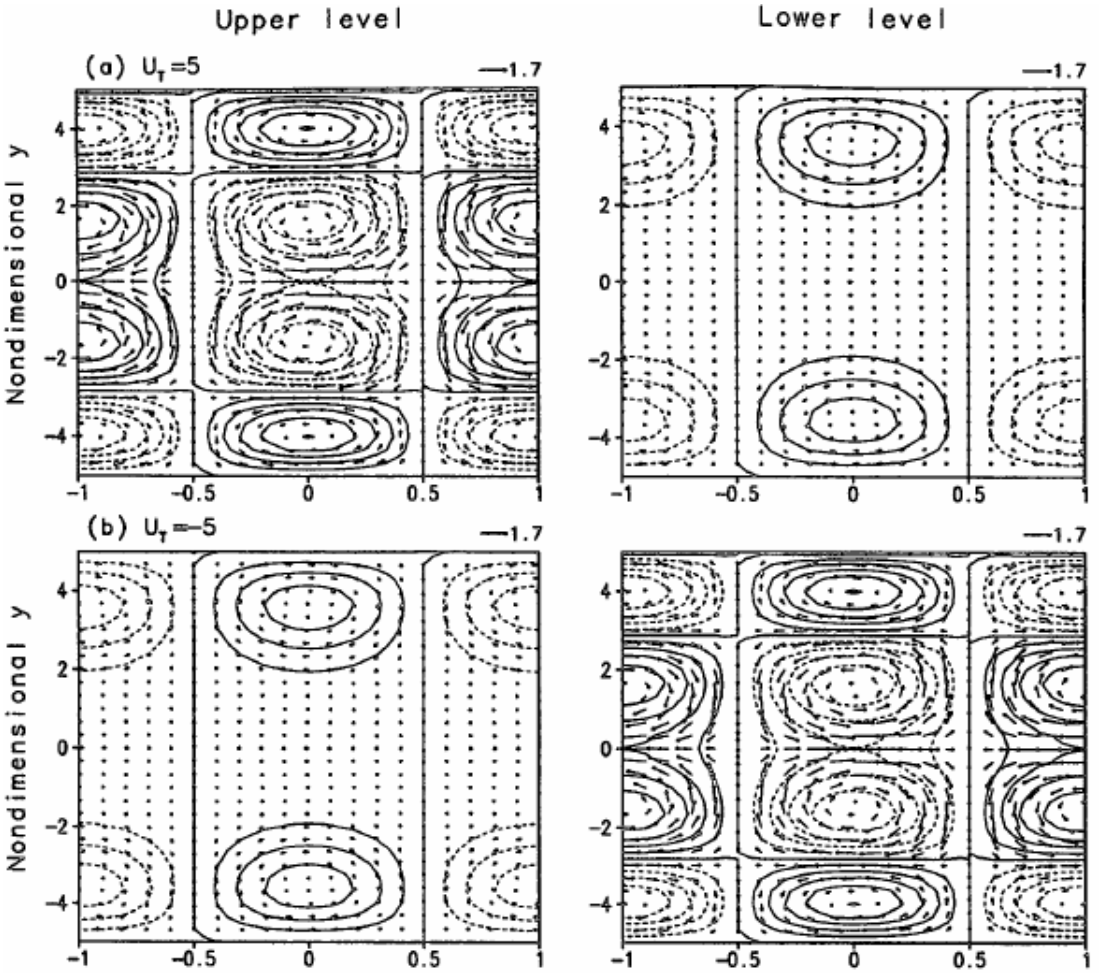

Fig. 9 Horizontal structure of the n=1 Rossby waves with a wavelength of 10,000 km. Geopotential and wind patterns in the upper and lower troposphere are displayed for (a) U =5 m/s (westerly vertical shear) and (b) U_T= -5 m/s (easterly vertical shear). The abscissa denotes zonal phase in units of π. Adopted from Wang and Xie (1996).

Figure 9 presents three-dimensional structure of the n=1 Rossby waves in a westerly vertical shear (Fig. 9a) and an easterly vertical shear (Fig. 9b) in comparison with the case without the vertical shear (Fig. 9c). In a westerly (easterly) shear, the Rossby waves have larger amplitude at the upper (lower) troposphere. This is particularly evident in the tropical regions. Poleward about two Rossby radii of deformation, the barotropic mode dominates and the sign of the geopotential perturbation there tends to be out of phase with that in the tropical region. Obviously, the vertical shear has changed the vertical structure of the Rossby wave drastically. The reason is that the nature of coupling of the two vertical modes depends on the sign of the vertical shear (A.3.3 and A.3.4). Wang and Xie (1996) has shown that for a constant vertical shear, one of the vertical modes may have a structure that is independent of the sign of the shear, but the remaining mode must

then have a structure that is dependent of the sign of the vertical shear. However, no matter which mode is assumed to be independent of the sign of the vertical shear the two vertical modes are in phase in the westerly shears, whereas they are 180^o out of phase in easterly shears. Thus, the vertical shear creates a vertical asymmetry in the Rossby wave structure.

The presence of vertical shears also slows down the westward propagation of the Rossby waves regardless of the sign of the vertical shear. The reason is that Rossby waves tend to reside in the westerlies and have an elevated (lowered) steering flow level for the Rossby waves in a westerly (easterly) shear. If the vertical mean zonal flow vanishes, the resultant mean zonal steering flow is thus eastward in both the westerly and easterly shears, which acts to reduce propagation speed of the Rossby waves.

The modification of the structure and propagation depends on strengths of the vertical shear and the wavelength. For a given shear, the structures of the short waves are more significantly modified and so are their phase speeds. In reality, the vertical shear of the zonal mean flow may also change with latitude. In the presence of meridional variation of the vertical shear, the Rossby waves will be enhanced in the vicinity of the latitudes where the vertical shear is strengthened, suggesting the importance of regional vertical shear in modification of the *in situ* wave characteristics.

The above discussion applies to stable Rossby waves. Further analysis has shown that vertical shear has profound influences on the instability of the moist equatorial Rossby waves (Xie and Wang 1996). When the vertical shear of the mean zonal flow exceeds certain critical value, the most trapped equatorial Rossby waves become unstable by extracting mean flow available potential energy. When convective heating is organized by and feedback to the equatorial Rossby waves, the preferred most unstable wavelength increases with increasing vertical shear and decreases with increasing heating intensity, ranging typically from 3000 to 5000 km.

Without boundary layer friction the Rossby wave instability does not depend on the sign of the vertical shear. However, in the presence of a boundary layer, easterly (westerly) shears enhance (suppress) the moist Rossby wave instability considerably. The reason is that an easterly shear confines the wave to the lower level, generating a stronger Ekman pumping-induced heating and meridional heat flux, both of which reinforce the instability. The opposite is true for a westerly shear. The effects of vertical shear on the westward propagating Rossby-Gravity waves are similar to those for Rossby waves. However, the vertical shear has little impacts on the equatorial Kelvin waves (Wang and Xie 1996).

3.2. Extratropical barotropic response induced by equatorial heating

One of the fundamental impacts of the vertical shear is excitation of prominent barotropic Rossby wave motion through interaction with the gravest baroclinic Rossby waves. This vertical shear mechanism may help explain how an equatorial heating generates a significant extratropical barotropic response.

An internal heating sitting on the equator can directly generate baroclinic Rossby mode (A.3.4). It can be shown from (A.3.3) that the vorticity equation of the barotropic mode is given by

$$\frac{D\zeta_+}{Dt} = -v_+ + U_T\left(\frac{\partial D_-}{\partial y} - \frac{\partial \zeta_-}{\partial x}\right). \tag{3.1}$$

Thus, the meridional variation of baroclinic divergence and longitudinal variation of the baroclinic vorticity acting on the vertical shear of the mean flow represents a source of forcing for the barotropic motion. Figures 9c and 8d show that the barotropic Rossby waves are not equatorially trapped; rather they have maximum amplitudes in the extratropics. Hence, an equatorial heating can indirectly generate extratropical barotropic Rossby waves, providing a mechanism by which equatorial heating can generate extratropical teleconnection patterns.

3.3. Asymmetric Rossby wave response to equatorial symmetric heating

In a resting atmosphere, an equatorial symmetric heating can only induce equatorial symmetric response in the pressure and zonal wind field. As discussed earlier, the vertical shear can induce remarkable equatorial asymmetry for the n=1 Rossby waves, which in the absence of the vertical shear has equatorial symmetric pressure and zonal winds. The Asian summer monsoon is characterized by significant vertical easterly shears over South Asia. Because the monsoon easterly shear is primarily confined to the NH, the unstable n=1 Rossby wave can become markedly trapped in the NH (Xie and Wang 1996). Under influence of such a summer mean monsoon circulation, even a heating that is symmetric about the equator can possibly induce considerably asymmetric Rossby wave response with major circulation located in the easterly vertical regions (i.e., the NH).

To validate the inference deduced from the theoretical model, a numerical experiment with an anomaly atmospheric general circulation model (AGCM) was performed (Wang et al. 2003). A multi-level linearized AGCM is chosen because more realistic three-dimensional basic states can be specified. 3-D summer (JJA) and winter (DJF) mean basic states were prescribed in an equally spaced five-level sigma coordinate. A strong momentum damping with a decaying time scale of one day is applied in the lowest model level to mimic the planetary boundary layer dissipation, while a Newtonian damping of e-folding time scale of 10 days is applied to all levels in both momentum and thermodynamic energy equations.

Figure 10 illustrates the response of the lowest-level winds to a prescribed ideal equatorial symmetric cooling. This cooling is motivated by mimicking the anomalous cooling associated with the maritime continent subsidence during El Nino. In the presence of the northern summer mean flow, the atmospheric response is obviously asymmetric to the equator: A strong low-level anticyclone anomaly appears to the north of the equator (Fig. 10a). The anomalous anticyclone extends to the west of the heat sink, covering the entire South Asian monsoon region. On the other hand, with specification of a resting background flow, the model produces a symmetric response with twin anticyclones residing on each side of the equator (figure omitted). When the mean winter (DJF) basic flow is specified, the model simulates a stronger anticyclonic response in the SH, consistent with the distribution of the easterly vertical shear (Fig. 10b). The numerical results shown in Fig. 10a provides an explanation why during ENSO developing phase the major monsoon anomalies are dominated by an anticyclonic ridge located north of the equator, while the response in the SH is weak (Wang et al. 2003). Using an intermediate atmospheric model, Wang and Xie (1997) identified the equatorial asymmetric response is primarily produced by the effects of the vertical shear in the seasonal mean state. During the mature phase of El Niño, the suppressed convection over the maritime continent and Australian monsoon region would favor anomalous

anticyclones forming over the tropical southern Indian Ocean, similar to the solution shown by Fig. 10b.

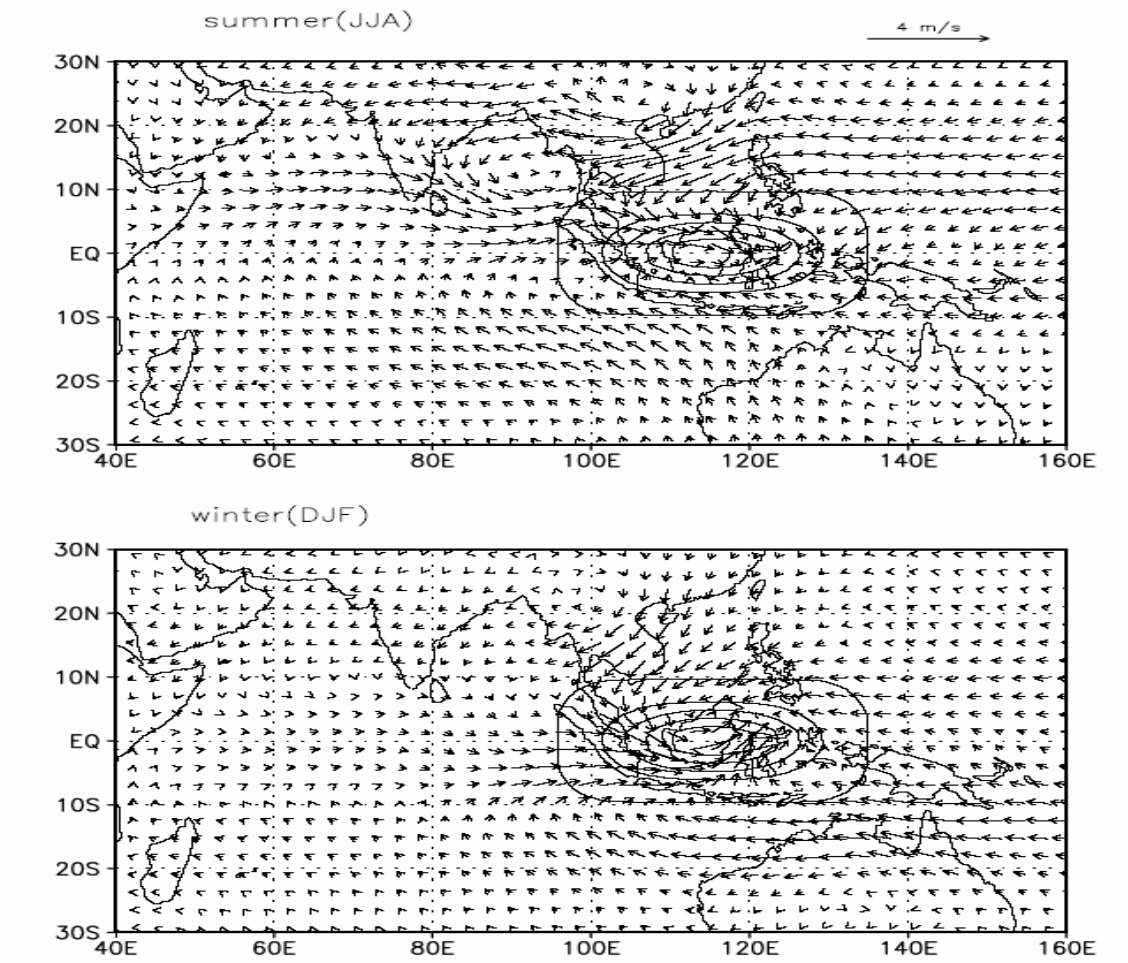

by using an anomaly atmospheric general circulation model with specified basic state of (a) boreal summer (JJA) mean and (b) boreal winter (DJF) mean climatological flow. The contours represent horizontal distribution of the heat sink strength at an interval of 0.4°C/day with maximum amplitude of the heating rate of –2 ºC/day, witch is located in the middle troposphere.

3.4. Wave energy accumulation in the equatorial westerly duct

One of the important impacts of the vertical shear on equatorial Rossby waves is that the westerly (easterly) shear favors trapping wave kinetic energy to the upper (lower) troposphere (Fig. 9). This may be pertinent to interpretation of the in-phase relationship between the transient kinetic energy and the equatorial mean flow in the upper troposphere as observed by Arkin and Webster (1985), which is also known as accumulation of wave energy in the upper tropospheric westerly duct (a zonal flow with westerly vertical shear). On the other hand, in a region of easterly vertical shear (monsoon regions), the Rossby waves tend to be trapped in the lower troposphere, which also agree with the behavior of perturbations in the summer monsoon trough region.

Appendix

A.1 Vertical modes and shallow water equations

a. Governing equations on the equatorial beta-plane

The Earth's rotational effects on dynamic processes in the tropics are most easily analyzed by utilizing an equatorial β-plane approximation, in which the Coriolis parameter $f = \beta y$, where $\beta \equiv df/dy = 2\Omega/a$ is the Rossby parameter with Ω and a the rotation rate and the radius of the Earth respectively.

The physical principles that govern the hydrostatic *perturbation* motion consist of conservations of momentum (A.1.1a,b), mass (A.1.1c), thermodynamic energy (A.1.1d), and water vapor (A.1.1e). These principles expressed in a vertical pressure (p) coordinates on an equatorial β-plane are

$$\frac{\partial u}{\partial t} + \beta y v = -\frac{\partial \phi}{\partial x} + F_x + N(u) \qquad \text{(A.1.1a)}$$

$$\frac{\partial v}{\partial t} - \beta y u = -\frac{\partial \phi}{\partial y} + F_y + N(v) \qquad \text{(A.1.1b)}$$

$$\frac{\partial u}{\partial x} + \frac{\partial v}{\partial y} + \frac{\partial \omega}{\partial p} = 0 \qquad \text{(A.1.1c)}$$

$$\frac{\partial}{\partial t}\frac{\partial \phi}{\partial p} + S(p)\omega = -\frac{R}{C_p p} Q_c(p) + N\left(\frac{\partial \phi}{\partial p}\right) \qquad \text{(A.1.1d)}$$

$$\frac{\partial}{\partial t} M_c + \frac{1}{g}\int_{p_u}^{P_s} \nabla \cdot (\bar{q}\vec{V}) dp = E_v - P_r + N(q) \qquad \text{(A.1.1e)}$$

In Eq. (A.1.1) (x, y) is the distance in the eastward and northward direction, the dependent variables, u, v, ω and ϕ, denote zonal and meridional wind, vertical pressure velocity, and geopotential height, respectively; F_x and F_y denote frictions and the terms $N(u)$, $N(v)$, $N(\partial\phi/\partial p)$, and $N(q)$ represent nonlinear advections. The static stability parameter $S(p)$ describes effects of atmospheric stratification; Q_c expresses diabatic heating rate per unit mass, and R and C_p are the gas constant of the air and the specific heat at constant pressure, respectively. More detailed explanation of diabatic heating and moisture eq. (A.1.1e) will be given in section A.4.

b. The vertical mode and the shallow water equation

To better understand the three-dimensional, large-scale tropical atmospheric motion, it is helpful to begin with an idealized model in which the vertical structure of the "normal" modes can be determined and the corresponding horizontal motion can be described by simple equations. For this purpose, consider frictionless, dry, adiabatic and small amplitude perturbation motion in a quiescent environment, so that Eq.A.1.1 becomes:

$$\frac{\partial u}{\partial t} + \beta y v = -\frac{\partial \phi}{\partial x} \qquad \text{(A.1.2a)}$$

$$\frac{\partial v}{\partial t} - \beta y u = -\frac{\partial \phi}{\partial y} \tag{A.1.2b}$$

$$\frac{\partial u}{\partial x} + \frac{\partial v}{\partial y} + \frac{\partial \omega}{\partial p} = 0 \tag{A.1.2c}$$

$$\frac{\partial}{\partial t}\frac{\partial \phi}{\partial p} + S(p)\omega = 0 \tag{A.1.2d}$$

Because the static stability parameter *S* varies primarily in the vertical direction, let us assume $S(p)$ is a function of pressure only that can be quite well approximated by $S(p) = C_s{}^2 / p^2$. Here $C_s = p_s S(p_s)^{1/2}$ represent a reference gravity wave speed at the surface $p = p_s$, which is about 70 m/s for typical dry tropical atmosphere. Then the solutions of (A.1.2) can be expressed as

$$\omega = \Omega \cdot W(p) \tag{A.1.3a}$$

$$(u, v, \Phi) = (U, V, \Phi)\frac{dW}{dp}(p) \tag{A.1.3b}$$

where *W (p)* describe the vertical structure of the motion, whereas *U*, *V*, Φ , and Ω are only functions of *x*, *y*, *and t*. Substituting (A.1.3) into (A.1.2), one finds that the *W(p),* satisfies

$$C^2 \frac{d^2 W}{dp^2} + S(p)W = 0 \tag{A.1.4}$$

and the horizontal motion *U*, *V*, Φ , satisfy

$$\frac{\partial U}{\partial t} - \beta y V = -\frac{\partial \Phi}{\partial x} \tag{A.1.5a}$$

$$\frac{\partial V}{\partial y} + \beta y U = -\frac{\partial \Phi}{\partial y} \tag{A.1.5b}$$

$$\frac{\partial \Phi}{\partial x} + C_0^2\left(\frac{\partial U}{\partial x} + \frac{\partial V}{\partial y}\right) = 0 \tag{A.1.5c}$$

where C_0^2 is a 'separation constant'. Eq. (A.1.5) describe horizontal wave propagation and is referred to as 'shallow water equation' because it is similar to the equation that describes the propagation of the long gravity surface waves with a speed C_0 .

Of note is that the vertical structure of atmospheric motion may be expressed in terms of the sum of many vertical 'normal' modes. For simplicity, assume an atmosphere being confined by a lower surface at $p=p_s$ and a 'lid' at the tropopause, $p=p_u$ at which we impose $\omega=0$. The normal mode solution of (A.1.4) with the given boundary conditions yields (A.1.6) a family of infinite number of vertical modes $W_m(p)$ with an arbitrary amplitude A_m (Wang and Chen 1989):

$$W_m(p) = Am(p^{1/2+b_m} - p_u^{2b_m} p^{1/2-b_m}),\ \text{m= 1, 2, 3…} \tag{A.1.6}$$

where

$$b_m = im\pi(\ln p_s / p_u) \quad . \tag{A.1.6a}$$

The phase speed corresponding to the m[th] vertical mode is

$$C_0(m) = C_s(1/4 - b_m^2)^{-1/2} \quad . \tag{A.1.7}$$

We note that the vertical structures and the gravity wave phase speed of each vertical mode are solely determined by the basic state stratification.

A.2 Equatorial waves

Using $Rc = (C_0/\beta)^{1/2}$ (the equatorial Rossby radius of deformation), $\tau = (\beta C_0)^{-1/2}$, and C_0^2 as characteristic scales for the horizontal length, time, and geopotential height, respectively, one can obtain the following non-dimensional shallow water equation for description of a single vertical mode

$$\frac{\partial u'}{\partial t'} - y'v' = -\frac{\partial \phi'}{\partial x'} \ , \tag{A.2.1a}$$

$$\frac{\partial v'}{\partial t'} + y'u' = -\frac{\partial \phi'}{\partial y'} \ , \tag{A.2.1b}$$

$$\frac{\partial \phi'}{\partial t'} + \frac{\partial u'}{\partial x'} + \frac{\partial v'}{\partial y'} = 0 \ . \tag{A.2.1c}$$

where the prime denotes non-dimensional quantities. The dimensional variables may be returned by multiplication of their corresponding characteristic scales.

Consider first the wave motion without meridional wind (Kelvin waves). The system of equation (A.2.1) becomes

$$\frac{\partial u'}{\partial t'} = -\frac{\partial \phi'}{\partial x'} \tag{A.2.2a}$$

$$y'u' = -\frac{\partial \phi'}{\partial y'} \tag{A.2.2b}$$

$$\frac{\partial \phi'}{\partial t'} + \frac{\partial u'}{\partial x'} = 0 \tag{A.2.2c}$$

The combination of (A.2.2a) and (A.2.2c) yields a wave equation, which has a general solution, $u' = F(x' \mp t')Y(y')$, where F is an arbitrary function. From (A.2.2a), $\phi' = \pm u'$. Using (A.2.2b), one can obtain $Y(y') = Y(0)e^{\mp y'^2/2}$. Only the minus sign is valid because the other choice leads to an unbounded solution for large y. The solution of the system is in dimensional form (A.2.3)

$$u = \phi / C_0 = F(x - C_0 t)e^{-\beta y^2/2C_0} \quad \text{and} \quad v \equiv 0 \tag{A.2.3}$$

In addition to the equatorial Kelvin wave solution, (A.2.1) has other equatorial wave solutions. Since the coefficients of (A.2.1) only depend on y, the solution for zonally propagating wave disturbance can be expressed as the form of normal modes

$$(u', v', \phi') = \mathrm{Re}(U(y), V(y), \Phi(y))e^{i(kx - \omega t)}$$

where 'Re' means taking real part, k is zonal wave number and ω the frequency which

assumed to be always positive so that $k>0$ implies eastward propagation relative to the ground with phase speed $C_x = \omega/k$, $U(y), V(y), \Phi(y)$ denotes the meridional structure and are assumed to be bounded, as $y \to \pm\infty$ (Matsuno 1966). This condition is necessary as the equatorial β-plane is not a valid approximation to spherical geometry for large y.

Substituting the normal mode solution into (A.2.1) and eliminate $U(y), \Phi(y)$ leads to an equation for *V(y):*

$$\frac{d^2V}{dy^2} + \left[(\omega^2 - k^2) - \frac{k}{\omega} - y^2 \right] V = 0 . \qquad \text{(A.2.4)}$$

Note that in deriving Equation (A.2.4), $k^2 \neq \omega^2$ was assumed, which excluded the equatorial Kelvin waves.

Equation (A.2.4) along with the boundary condition (*V(y)* is bounded as $y \to \pm\infty$) poses an eigenvalue problem, which is the same as the Schrödinger equation for a simple harmonic oscillator. Solution of Eq. (A.2.4) that satisfy the condition of equatorial trapping exist if and only if

$$\omega^2 - k^2 - k/\omega = 2n+1, \qquad n = 0, 1, 2,\ldots \qquad \text{(A.2.5)}$$

Equation (A.2.5) is the non-dimensional dispersion equation, which describes the relationship between the frequency ω and wavenumber k. Figure 3 shows the dispersion curve of the equatorial waves. When $n \geq 1$, the exact dispersion relation is given by

$$k_n = -\frac{1}{2\omega} \pm \sqrt{\omega^2 + 1/4\omega^2 - (2n+1)}, \quad n = 1, 2, 3,\ldots \qquad \text{(A.2.6)}$$

A real (number) k, which corresponds to propagating neutral waves (non-decaying), requires that either $\omega \geq \sqrt{(n+1)/2} + \sqrt{n/2} \geq 1 + 1/\sqrt{2}$ or $\omega \leq 1 - 1/\sqrt{2}$. Thus, there are two distinct groups of waves: one is high frequency waves, $\omega \geq 1 + 1/\sqrt{2}$ =1.71, and the other is low frequency waves, $\omega \leq 1 - 1/\sqrt{2}$ =0.29 (Fig. 3). When $n = 0$, the dispersion equation $\omega^2 - k^2 - k/\omega = 1$ yields only one meaningful root $k = \omega - 1/\omega$ (the curve $n = 0$ in Fig. 3).

Differentiating the dispersion equation, (A.2.5) with respect to k, one finds that the group speed in the x-direction is

$$C_{gx} \equiv \frac{\partial w}{\partial k} = \frac{2k\omega + 1}{2\omega^2 + k/\omega}$$

which vanishes at $2k\omega = -1$ (if $2\omega^2 + k/\omega \neq 0$). The curve $\omega = -1/2k$ is shown in Fig. 3 by the dashed line, which represents zero group speed.

The meridional structures of the zonal propagating Rossby, inertio-gravity and Rossby-gravity waves are described by the solutions of (A.2.4), which are the Weber-Hermite functions :

$$V(y) = D_n(y) = e^{-y^2/2} H_n(y), \; n = 0, 1, 2,\ldots \quad , \qquad \text{(A.2.7)}$$

where the $H_n(y)$ denotes the Hermite polynomial of order *n* (the meridional mode index)

$$H_n(y) \equiv \sum_{l=0}^{[n/2]} \frac{(-1)^l n!}{l!(n-2l)!} (2y)^{n-2l} \qquad . \qquad \text{(A.2.7a)}$$

The solutions for $U(y), \Phi(y)$ can be obtained from (A.2.1) in terms of (A.2.7).

The solution for the n=0 mode (the mixed Rossby-gravity waves), $k = \omega - 1/\omega$, and

the structure is given by

$$v_0' = \mathrm{Re}\, e^{-y^2/2} e^{i[(\omega - 1/\omega)x - \omega t]}, \tag{A.2.8a}$$

$$u_0' = \phi_0' = \mathrm{Re}\, i\omega e^{-y^2/2} y e^{i[(\omega - 1/\omega)x - \omega t]}. \tag{A.2.8b}$$

A.3 Theoretical model for study of mean flow effects on equatorial waves

Assume that the zonal mean flow $\bar{u}(p)$ satisfies geostrophic balance $\beta y \bar{u} = -\partial\phi/\partial y$. The equations governing inviscid, hydrostatic perturbation motions are (A.3.1), in which the meanings of the other symbols are the same as in (A.1.1) except $\bar{u}(p)$.

$$\frac{\partial u}{\partial t} + \bar{u}\frac{\partial u}{\partial x} + \omega\frac{\partial \bar{u}}{\partial p} - \beta y v = -\frac{\partial \phi}{\partial x} \tag{A.3.1a}$$

$$\frac{\partial v}{\partial t} + \bar{u}\frac{\partial v}{\partial x} + \beta y u = -\frac{\partial \phi}{\partial y} \tag{A.3.1b}$$

$$\frac{\partial u}{\partial x} + \frac{\partial v}{\partial y} + \frac{\partial \omega}{\partial p} = 0 \tag{A.3.1c}$$

$$\frac{\partial}{\partial t}\left(\frac{\partial \Phi}{\partial p}\right) + \bar{u}\frac{\partial}{\partial x}\left(\frac{\partial \phi}{\partial p}\right) - \beta y v \frac{\partial \bar{u}}{\partial p} + S\omega = 0 \tag{A.3.1d}$$

To illustrate basic mechanisms, a simple two-level model is adopted (Philips 1954). Writing the momentum and continuity equation (A.3.1a,b,c) at the upper (p_1) and lower (p_3) levels and the thermodynamic equation in the middle (p_m) level, one can obtain a set of governing equations in this two-level model. To facilitate elaboration of dynamic mechanisms, it is more convenient to introduce a barotropic and a baroclinic component (mode) defined by (A.3.2).

$$A_+ = (A_1 + A_3)/2\,,\ A_- = (A_1 - A_3)/2 \tag{A.3.2}$$

In (A.3.2), quantity A represents any dependent variable and A_+ and A_- are referred to as the corresponding barotropic and baroclinic mode, respectively. For the wind and geopotential fields, they describe, respectively, the vertical mean wind (geopotential) and the thermal wind (thickness). The governing equations are then written using the two vertical modes and are non-dimensionalized using the same scale as those used in deriving (A.2.1). In the two-level model, the internal gravity wave speed $C_m = \left(\Delta p^2 S_m/2\right)^{1/2}$.

Since the barotropic mode is nondivergent, a barotropic stream function Ψ can be introduced so that $u_+ = -\partial\psi/\partial y$ and $v_+ = \partial\psi/\partial x$. It can be shown that the barotropic stream function satisfies

$$\frac{D}{Dt}\nabla^2\psi + \frac{\partial \psi}{\partial x} = U_T\left(\frac{\partial^2}{\partial y^2} - \frac{\partial^2}{\partial x^2}\right)v_- + 2U_T\frac{\partial^2 u_-}{\partial x \partial y}, \tag{A.3.3}$$

where

$$\frac{D}{Dt} \equiv \frac{\partial}{\partial t} + \bar{U}\frac{\partial}{\partial x}, \tag{A.3.3a}$$

$$\bar{U} = \left(\bar{u_1} + \bar{u_3}\right)/2\,,\quad U_T = \left(\bar{u_1} - \bar{u_3}\right)/2\,. \tag{A.3.3b}$$

The baroclinic mode is governed by (A.3.4).

$$\frac{Du_-}{Dt} - yv_- + \frac{\partial \phi_-}{\partial x} = -U_T \frac{\partial u_+}{\partial x}, \tag{A.3.4a}$$

$$\frac{Dv_-}{Dt} + yu_- + \frac{\partial \phi_-}{\partial y} = -U_T \frac{\partial v_+}{\partial x}, \tag{A.3.4b}$$

$$\frac{\partial \phi_-}{\partial x} + \frac{\partial u_-}{\partial x} + \frac{\partial v_-}{\partial y} = yv_+ U_T . \tag{A.3.4c}$$

A.4 An one and one half layer model including interactive diabatic heating

Representation of interactive diabatic heating is an extremely challenging problem. Here we try to represent the convective heating effect in a rudimentary way, mainly for the convenience of theoretical analysis. This model, as will be shown, is an extension of Matsuno model that includes diabatic heating and boundary layer dynamics.

In the thermodynamic equation (A.1.1d), two diabatic heating terms are included: the condensational latent heat and a simplest form of radiation cooling, Newtonian cooling, with a constant coefficient μ. The condensational heating rate Q_c must be constrained by precipitation rate, i.e., the column integrated condensational heating rate is linked with the precipitation rate:

$$\delta L_c P_r = \frac{1}{g}\int_{p_u}^{p_s} Q_c(p)\,dp , \tag{A.4.1}$$

where L_c is latent heat of condensation and δ represents a switch-on tracer for nonlinear heating in the absence of basic state rainfall: δ equals unity in region of positive precipitation and zero otherwise. The heating is linear when $\delta \equiv 1$.

Equation (A.1.1e) describes the conservation of water vapor, which requires the local rate of change in the column-integrated water vapor M_c, to be balanced by the sum of the column integrated moisture convergence, perturbation precipitation rate P_r and the perturbation surface evaporation rate E_v. In the moisture convergence term, $\vec{V}$ represents the horizontal wind and p_u and p_s are the pressures at the upper and lower boundary, respectively. The moisture convergence depends on the basic state specific humidity, $\overline{q}$, which provides latent energy for the perturbation motion. We assume that the absolute humidity of the basic state atmosphere falls off with height exponentially with a water scale height H_1=2.2km. The mean specific humidity in an arbitrary vertical layer between pressure p_1 *and* p_2 where $p_2 > p_1$ is (Wang, 1988):

$$\overline{q}(p_1, p_2) = q_0 \frac{\left(p_2^m - p_1^m\right)}{m(p_2 - p_1)}, \tag{A.4.2}$$

where $m = H/H_1$ is the ratio of the density scale height H to the water vapor scale height, H_1, and q_0 is the air specific humidity at the surface. Over ocean and on the time scale of a few weeks and longer, q_0 is well correlated with *SST* and may be approximated by the following empirical formula (Li and Wang 1994):

$$q_0 = q_0(SST) = \left(0.94 \times SST\left(^oC\right) - 7.64\right) \times 10^{-3} . \tag{A.4.2a}$$

Since large-scale tropical motion is stimulated by condensational heating in the middle troposphere, the vertical structure of the motion is dominated by the gravest baroclinic mode. Thus, the simplest model should consist of two layers in the free troposphere. In

the absence of basic flows, all advection terms in Eq. A.1.1 can be neglected for perturbation motion. As shown in section A.3, the motion in the two-level free atmosphere can be represented by a baroclinic and a barotropic mode. In the presence of boundary layer friction, these two vertical modes are coupled through frictional convergence induced vertical motion at p_e, the top of the boundary layer. To save space, the equations for this two-level system are not given here. The interested readers can find them, e.g., in Wang and Rui (1990). Note that only the baroclinic mode is subjected to diabatic heating. The condensational heating is linked to the precipitation rate (Eq. A.4.1). With the limited vertical resolution of the 2-level system, the precipitation rate is expressed by

$$\delta P_r' = \delta b\{[-\omega_2 \bar{q}_3 - \omega_e(\bar{q}_e - \bar{q}_3)]/g + \rho_s C_E |V_b|(q_s - q_0)\}, \tag{A.4.3}$$

where ω_e and ω_2 represent, respectively, vertical pressure velocities at the top of the boundary layer (p_e) and the mid troposphere (p_2); g, ρ_s, and C_E are gravity, surface air density, and heat exchange coefficient, respectively; V_b the wind speed at surface $p = p_s$ that will be approximated by the model boundary-layer wind; q_s the saturation specific humidity at the sea surface temperature, which can be calculated from the Clausius-Clapeyron equation. Equation (A.4.3) enables the governing equations be a closed system.

It has been demonstrated that *in the absence of basic flows* the magnitude of the barotropic mode is an order of magnitude smaller than that of the baroclinic mode (Wang and Rui 1990, Wang and Li 1993). Thus, a simplification can be made to neglect the barotropic mode by assuming a vanishing column integral of divergence in the free troposphere. The baroclinic mode in the free troposphere is then governed by the following equations on an equatorial β-plane (after ω_2 and ω_e are eliminated by using continuity equation):

$$\frac{\partial u}{\partial t} + \beta y v = -\frac{\partial \phi}{\partial x}, \tag{A.4.4a}$$

$$\frac{\partial v}{\partial t} - \beta y u = -\frac{\partial \phi}{\partial y}, \tag{A.4.4b}$$

$$C_0^{-2}\frac{\partial \phi}{\partial t} + (1-\delta I)\nabla\cdot\vec{V} = d(\delta B - 1)\nabla\cdot\vec{V}_b - \delta F C_E |\vec{V}_b|/h, \tag{A.4.4c}$$

where u, v and ϕ represent the lower-troposphere zonal and meridional wind and geopotential height, respectively (the upper-tropospheric zonal and meridional wind are $-u$ *and* $-v$, respectively); $\vec{V}_b$ denotes boundary layer barotropic wind whose components (u_b, v_b) satisfy a linear version; C_0 = 50 m/s denotes dry gravity wave speed of the free-troposphere baroclinic mode (corresponding to the gravest baroclinic mode in a vertically continuous model); $d = (p_s - p_e)/\Delta p$ is the dimensionless depth of the boundary layer; and $h = \Delta p/\rho_e g$, where Δp is one-half pressure depth of the free troposphere. In the thermodynamic equation (A.4.4c) there are three non-dimensional heating parameters, which are defined by

$$I = \bar{q}_3 / q_c \quad \text{Heating coefficient due to wave convergence,} \tag{A.4.5a}$$

$$B = \bar{q}_e / q_c \quad \text{Heating coefficient due to frictional convergence,} \tag{A.4.5b}$$

$$F = (q_s - q_0)/q_c \quad \text{Heating coefficient associated with evaporation,} \tag{A.4.5c}$$

where $q_c = 2C_p p_s C_0^2/(bR\Delta pL_c)$ stands for a vertical mean specific humidity in the lower-tropospheric layer, corresponding to a vanishing effective static stability in the presence of convective heating. The standard values of model parameters used in this chapter are the same as in Wang and Li (1994).

Note that, in a two-level free atmospheric model, the heating is released in the middle of the troposphere; the closure assumption for condensational heating is provided solely by conservation laws for moisture and thermal energy through the linkage between vertical integrated condensational heating rate and the precipitation rate in the same column (A.4.1). Any type of cumulus parameterization, when reduced to a two-level approximation, must obey the same physical principles. Therefore, use of (A.4.3) should not be considered a version of Kuo or any other specific parameterization schemes. The only approximation made in (A.4.3) is the neglect of the local change of moisture and the moisture in the upper-tropospheric layer. An adjustable parameter, *b*, is introduced to compensate the omission of the moisture storage in the atmosphere. The parameter *b* represents the condensation efficiency measuring the fraction of total moisture convergence that condenses out as precipitation. This simplification facilitates eigenvalue analysis. A two-level version of the time-dependent moisture equation (A.1.1e) and a transient boundary layer (rather than steady boundary layer) had also been used; the results are not qualitatively different from those derived with these simplifications.

The equations (A.4.4a-c) and (A.4.5a,b) (with the assumption $\phi_e = \phi$) consist of a closed set of equations, which describes moist dynamics of a single free troposphere baroclinic mode that is coupled with the boundary-layer motion.. Such a model is referred to as a one and one half (1-1/2) layer model.

Acknowledgment. Much of the materials presented here come from a book chapter in "Asian Monsoon": Hoskins and Wang 2005: Large scale dynamics, Chapter 9 in "Asian Monsoon" Ed. Bin Wang, Springer-Praxis, New York, pp357-416.

References

Arkin, P. A. and P. J. Webster, 1985: Annual and interannual variability of tropical-extratropical interaction: An empirical study. *Mon. Wea. Rev.*, **113**, 1510–1523.

Bjerknes, J., 1966: A possible response of the atmospheric Hadley circulation to equatorial anomalies of ocean temperature. *Tellus*, **18**, 820-829.

Charney, J. G. and A. Eliassen, 1964: On the growth of the hurricane depression. *J. Atmos. Sci.*, **21**, 68-75.

Eliassen. A., 1971: On the Ekman layer in a circular vortex. *J. Meteorol. Soc. Japan*, **49** (special issure), 784-789.

Emanuel, K. A., 1987: An air-sea interaction model of intraseasonal oscillation in the tropics. *J. Atmos. Sci.*, **44**, 2324-2340.

Gill, A. E., 1980: Some simple solutions for heat-induced tropical circulation. *Quart. J. R. Met. Soc.*, **106**, 447-462.

Hendon H. H., M. L. Salby, 1994: The life cycle of the Madden–Julian oscillation. *J. Atmos. Sci.*, **51**, 2225–2237

Hu, Q. and D. A. Randall, 1995: Low-frequency oscillation in radiative-convective systems. *J. Atmos. Sci.*, **52**, 478-490.

Hoskins, B. J., and F. Jin, 1991: The initial value problem for tropical perturbations to a baroclinic atmosphere. *Quart. J. Roy. Meteor. Soc.,* 117, 299-317.

Jiang, X. N., T. Li, and B. Wang, 2004: Structures and mechanisms of the northward propagating boreal summer intraseasonal oscillation. *J. Climate*, **17**, 1022–1039.

Kasahara, A. and P. L. Silva Dias, 1986: Response of planetary waves to stationary tropical heating in a global atmosphere with meridional and vertical Shear. *J. Atmos. Sci.*, **43**, 1893–1912.

Lau, K. H., and N. C. Lau, 1990: Observed structure and propagation characteristics of tropical summertime synoptic scale disturbances. *Mon. Wea. Rev.* **118**, 1888–1913.

Lim, H. and C. P. Chang, 1986: Generation of internal-and external-mode motions from internal heating: Effects of vertical shear and damping. *J. Atmos. Sci.*, **43**, 948–960.

Lin, J.-L., and B. E. Mapes, 2004: Radiation budget of the tropical intraseasonal oscillation. *J. Atmos. Sci.*, **61**, 2050-2062.

Lindzen, R. S., 1974: Wave-CISK in tropics. *J. Atmos. Sci.*, **31**, 156-179.

Lindzen, R. S., and S. Nigam (1987), On the role of the sea surface temperature gradients in forcing low-level winds and convergence in the Tropics, *J. Atmos. Sci., 44*, 2440–2458.

Liu, Y. M., G. X. Wu, H. Liu, and P. Liu, 2001: Dynamical effects of condensation heating on the subtropical anticyclones in the Eastern Hemisphere. *Climate Dyn.,* **17**, 327-338.

Lorenz, E. N., 1967: The nature and theory of the general circulation of the atmosphere. Tech. Doc. 218, World Meteorological Organization, 161 pp.

Madden, R. A. and P. R. Julian, 1972: Description of large-scale circulations cells in the tropics with a 40-50 day period, *J. Atmos. Sci.*, **29**, 1109-1123.

Mapes. B. E., 2000: Convective inhibition, subgrid-scale triggering energy, and stratiform instability in a toy tropical wave model. *J. Atmos. Sci.*, **57**, 1515-1535.

Matsuno, T., 1966: Quasi-geostrophic motions in the equatorial area. *J. Meteor. Soc. Japan*, **44**, 25-42.

Neelin, J. D. and I. M. Held, 1987: Modeling tropical convergence based on the moist static energy budget. *Mon. Wea. Rev.*, **115**, 3-12.

Neelin, J. D., I. M. Held and K. H. Cook, 1987: Evaporation-wind feedback and low-frequecy variability in the tropical atmosphere. *J. Atmos. Sci.*, **44**, 2341-2348.

Neelin, J. D., and J. Y. Yu, 1994: Modes of tropical variability under convective adjustment and Madden-Julian oscillation. 1: Analytical theory. *J. Atmos. Sci.*, **51**, 1876-1894.

Ooyama, K., 1964: A dynamic model for the study of tropical cyclone development. *Geofits. Int.*, 4, 187-198.

Raymond, D. J., 2001: A new model of the Madden-Julian oscillation. *J. Atmos. Sci.*, **58**, 2807-2819.

Rui., H., and B. Wang, 1990: Development characteristics and dynamic structure of the tropical intraseasonal convective anomalies. *J. Atmos. Sci.*, **47**, 357-379.

Wang, B., 1988: Dynamics of tropical low-frequency waves: an analysis of the moist Kelvin wave. *J. Atmos. Sci.,* **45,** 2051-2065.

Wang, B., 2005: theories. In: K. M. Lau and D. E. Waliser (eds), *Intraseasonal variability of the Atmosphere-Ocean Climate System*. Springer-Verlag, Heidelberg, Germanny.

__, and J. K. Chen, 1989: On the zonal-scale selection and vertical structure of equatorial intraseasonal waves. *Quart. J. Roy. Meteorol. Soc.*, **115**, 1301-1323.

__, and T. Li, 1993: A simple tropical atmosphere model of relevance to short-term climate variations. *J. Atmos. Sci.,* **50,** 260-284.

__, and __, 1994: Convective interaction with boundary-layer dynamics in the development of a tropical intraseasonal system. *J. Atmos. Sci.,* **51**, 1386-1400.

__, and H. Rui, 1990a: Dynamics of the coupled moist Kelvin-Rossby wave on an equatorial beta -plane. *J. Atmos. Sci.,* **47,** 397-413.

__, and X. Xie, 1996: Low-frequency equatorial waves in vertically sheared zonal flow. Part I: Stable waves. *J. Atmos. Sci.,* **53**, 449-467.

__, and __, 1997: A model for the boreal summer intraseasonal oscillation. *J. Atmos. Sci.,* **54,** 72-86.

__, and __, 1998: Coupled modes of the warm pool climate system. Part I: The role of air-sea interaction in maintaining Madden-Julian Oscillation. *J. Atmos. Sci.,* **11**, 2116-2135.

__, R. G. Wu, and T. Li, 2003: Atmosphere–warm ocean interaction and its impacts on Asian–Australian monsoon variation. *J. Climate*, **16**, 1195–1211.

Webster, P. J. 1972: Response of the tropical atmosphere to local steady forcing. *Mon. Wea. Rev.*, **100**, 518–541.

Wilson, J. D.and M. Mak, 1984: Tropical response to lateral forcing with a latitudinally and zonally nonuniform basic state. *J. Atmos. Sci.,* **41**, 1187–1201.

Woolnough, S.J., Slingo, J.M. and Hoskins, B.J., 2001: The organisation of tropical convection by intraseasonal sea surface temperature anomalies. Q.J.R. Meteorol. Soc., **127**, 887-907.

Wu, G. X., Y. M. Liu, and P. Liu, 1999: Spatially inhomogeneous diabatic heating and its impacts on the formation and variation of subtropical anticyclone, I: Scale Analysis. *Acta. Meteor. Sin*., **57**, 257-263.

Xie, X. S. and B. Wang, 1996: Low-frequency equatorial waves in vertically sheared zonal flow. Part II: Unstable waves. *J. Atmos. Sci.*, **53**, 3589–3605.

Yamasaki, M., 1969: Large-scale disturbances in conditionally unstable atmosphere in low latitudes. *Papers in Meteorology and Geophysics,* **20**, 289-336.

Yang, G.-Y., Hoskins, B.J. and Slingo, J.M., 2003: A new methodology for identifying wave structures in observational data. J. Atmos. Sc., **60**, 1637-1654.